THE JOURNAL OF BIOLOGICAL CHEMISTRY
Vol. 279, No. 35, Issue of August 27, pp. 37030–37039, 2004

Printed in U.S.A.

Enrichment of Endoplasmic Reticulum with Cholesterol Inhibits Sarcoplasmic-Endoplasmic Reticulum Calcium ATPase-2b Activity in Parallel with Increased Order of Membrane Lipids

IMPLICATIONS FOR DEPLETION OF ENDOPLASMIC RETICULUM CALCIUM STORES AND APOPTOSIS IN CHOLESTEROL-LOADED MACROPHAGES*

Received for publication, May 10, 2004, and in revised form, June 21, 2004
Published, JBC Papers in Press, June 23, 2004, DOI 10.1074/jbc.M405195200

Yankun Li‡, Mingtao Ge§, Laura Ciani§¶, George Kuriakose‡, Emily J. Westover‖, Miroslav Dura, Douglas F. Covey‖, Jack H. Freed§, Frederick R. Maxfield‡‡, Jonathan Lytton§§¶¶, and Ira Tabas‡‖‖**

*From the ‡Departments of Medicine, Anatomy & Cell Biology, and Physiology and Cellular Biophysics and the **Center for Molecular Cardiology, Columbia University, New York, New York 10032, the §Department of Chemistry and Chemical Biology, Baker Laboratory, Cornell University, Ithaca, New York 14853, the ‖Department of Molecular Biology and Pharmacology, Washington University School of Medicine, St. Louis, Missouri 63110, the ‡‡Department of Biochemistry, Weill Medical College of Cornell University, New York, New York 10021, and the §§Department of Biochemistry and Molecular Biology, University of Calgary Health Sciences Center, Calgary, Alberta T2N 4N1, Canada*

Macrophages in advanced atherosclerotic lesions accumulate large amounts of unesterified, or "free," cholesterol (FC). FC accumulation induces macrophage apoptosis, which likely contributes to plaque destabilization. Apoptosis is triggered by the enrichment of the endoplasmic reticulum (ER) with FC, resulting in depletion of ER calcium stores, and induction of the unfolded protein response. To explain the mechanism of ER calcium depletion, we hypothesized that FC enrichment of the normally cholesterol-poor ER membrane inhibits the macrophage ER calcium pump, sarcoplasmic-endoplasmic reticulum calcium ATPase-2b (SERCA2b). FC enrichment of ER membranes to a level similar to that occuring *in vivo* inhibited both the ATPase activity and calcium sequestration function of SERCA2b. Enrichment of ER with *ent*-cholesterol or 14:0–18:0 phosphatidylcholine, which possess the membrane-ordering properties of cholesterol, also inhibited SERCA2b. Moreover, at various levels of FC enrichment of ER membranes, there was a very close correlation between increasing membrane lipid order, as monitored by 16-doxyl-phosphatidycholine electron spin resonance, and SERCA2b inhibition. In view of these data, we speculate that SERCA2b, a conformationally active protein with 11 membrane-spanning regions, loses function due to decreased conformational freedom in FC-ordered membranes. This biophysical model may underlie the critical connection between excess cholesterol, unfolded protein response induction, macrophage death, and plaque destabilization in advanced atherosclerosis.

The cholesterol-loaded macrophage, or foam cell, is a hallmark of atherosclerotic lesions (1, 2). Cholesterol accumulates in these cells as a result of the internalization of arterial-wall lipoproteins (3). In early atherosclerosis, most of the lipoprotein-derived cholesterol is esterified to fatty acids by the enzyme acyl-CoA:cholesterol acyltransferase (ACAT), which is localized in the endoplasmic reticulum (ER) (4). In late lesions, however, macrophages accumulate mostly unesterified, or "free," cholesterol (FC) (5, 6). Although the mechanism of FC accumulation is not known, there is evidence *in vivo* to suggest that ACAT[1] dysfunction, likely coupled with defects in cellular cholesterol efflux, contribute to this process (7). Most importantly, FC accumulation in late lesional macrophages induces apoptosis and secondary necrosis in these cells (7). These events are thought to contribute to lesional necrosis and to promote plaque disruption, which in turn leads to acute atherothrombotic cardiovascular events (7, 8). Thus, an important goal in this area of research is to understand the mechanisms of cholesterol-induced cytotoxicity in FC-loaded macrophages.

In this context, recent work in our laboratory has begun to elucidate the cellular and molecular events involved in FC-induced apoptosis. The key event appears to be induction of the ER stress pathway known as the unfolded protein response (UPR) (9). One of the effector molecules of the UPR, a transcription factor called CHOP (GADD153), has been implicated in a number of apoptotic pathways (10, 11), and we have shown that macrophages from *Chop*$^{-/-}$ mice are resistant to FC-in-

* This work was supported in part by National Institutes of Health Grants HL75662 and HL54591 (to I. T.), HL57560 (to I. T. and F. R. M.), RR016292 and GM25862 (to J. H. F.), Cardiovascular Research Training Grant 55935 (to E. J. W.), National Institutes of Health Grant GM47969 (to D. F. C.), research support from the Heart & Stroke Foundation of Alberta, NWT, and Nunavut (to J. L.), and the University of Florence and the Italian Consorzio Sistemi a Grande Interfase (to L. C.). The costs of publication of this article were defrayed in part by the payment of page charges. This article must therefore be hereby marked "*advertisement*" in accordance with 18 U.S.C. Section 1734 solely to indicate this fact.

¶ Current address: Dept. of Chemistry, University of Florence, Firenze, Italy.

¶¶ Senior Scholar of the Alberta Heritage Foundation for Medical Research and an Investigator of the Canadian Institutes of Health Research.

‖‖ To whom correspondence and reprint requests should be addressed: Dept. of Medicine, Columbia University, 630 West 168th St., New York, NY 10032. Tel.: 212-305-9430; Fax: 212-305-4834; E-mail: iat1@columbia.edu.

[1] The abbreviations are: ACAT, acyl-CoA:cholesterol acyltransferase; 16-doxyl-PC, 1-palmitoyl-2-stearoyl(16–4′,4-dimethyloxazlidin-*N*-oxy)-*sn*-glycero-3-phosphocholine; DPPC, dipalmitoyl phosphatidylcholine; ER, endoplasmic reticulum; FC, free cholesterol; LDL, low density lipoprotein; MβCD, methyl-β-cyclodextrin; PC, phosphatidylcholine; SERCA, sarcoplasmic-endoplasmic reticulum calcium ATPase; UPR, unfolded protein response; FBS, fetal bovine serum; PBS, phosphate-buffered saline; MOPS, 4-morpholinepropanesulfonic acid.

duced apoptosis (9). Moreover, genetic and pharmacologic manipulations that block FC trafficking to the ER block both CHOP induction and apoptosis. Thus, FC trafficking to the ER somehow induces the UPR, and the CHOP branch of the UPR then leads to the induction of apoptosis pathways in these cells. In the *Apoe*$^{-/-}$ mouse model of atherosclerosis, FC-rich macrophages in advanced atherosclerotic lesions express CHOP, and inhibition of FC trafficking to the ER blocks lesional macrophage apoptosis and lesional necrosis (9, 12).

How might FC trafficking to the ER induce the UPR? We have shown that the earliest detectable event in the FC-UPR-apoptosis pathway is depletion of ER calcium stores (9). Low calcium in the ER lumen is a known inducer of the UPR, most likely by causing dysfunction of calcium-dependent protein chaperones such as calreticulin, calnexin, and BiP (13, 14). Proof for this connection in FC-loaded macrophages must await future experiments in which ER calcium pools could somehow be maintained in FC-loaded macrophages. However, pending such proof, we sought to explore how FC loading of the ER might lead to ER calcium depletion.

A critical molecule involved in the maintenance of ER calcium stores is sarcoendoplasmic reticulum calcium ATPase (SERCA), which pumps calcium from the cytosol into the ER lumen (15). The SERCA family is encoded by three distinct genes, numbered 1–3, each of which has multiple isoforms (16–18). Although these SERCA isoforms have similar overall structures and function, there are differences in certain specific structural features, functional characteristics, and regulatory properties (19). Most notably, certain isoforms are only expressed in muscle, which contains abundant sarcoplasmic reticulum and high SERCA expression. Specifically, SERCA1a and -1b are expressed exclusively in fast-twitch skeletal muscle, SERCA2a is expressed in cardiac and slow-twitch skeletal muscle, and SERCA2b, -3a, and -3b are expressed in non-muscle cells (20).

We now report that FC loading of ER membranes containing SERCA2b, the form found in macrophages, profoundly inhibits SERCA2b ATPase activity and calcium sequestration. Moreover, this inhibition is directly correlated with an increase in order parameter of the ER membrane, which is normally relatively fluid (21). Although previous studies have investigated similar questions with skeletal muscle SERCA1, the results of those studies have been somewhat variable, and, most importantly, not related to a specific physiological or pathophysiological event *in vivo* (see "Discussion"). In the current study, the increase in the FC:phospholipid ratio needed to change fluidity and inhibit SERCA2b in the range that occurs *in vivo* during FC loading of macrophages. These findings support the hypothesis that FC trafficking to the ER, by increasing lipid packing of this normally fluid membrane, inhibits SERCA2b activity. This series of events likely contributes to ER calcium depletion in FC-loaded macrophages and may be a critical event in the induction of the UPR and FC-induced apoptosis.

EXPERIMENTAL PROCEDURES

Materials—Tissue culture media and reagents were from Invitrogen. High performance liquid chromatography grade organic solvents were purchased from Fisher Scientific. Cholesterol and other sterols were obtained from Steraloids. Synthetic phospholipids, including the spin label 16-doxyl-PC (1-palmitoyl-2-stearoyl[16-doxyl]-*sn*-glycero-3-phosphocholine, where doxyl refers to 4′,4-dimethyloxazlidin-*N*-oxy) were obtained from Avanti Polar Lipids (Alabaster, AL). *Ent*-cholesterol was synthesized as previously described (22). Low density lipoprotein (LDL; *d* 1.020–1.063 g/ml) was isolated from fresh human plasma by preparative ultracentrifugation (23). Acetyl-LDL was prepared by reaction of LDL with acetic anhydride (24). Compound 58035 (3-[decyldimethylsilyl]-*N*-(2-(4-methylphenyl)-1-phenylethyl)propanamide), an inhibitor of ACAT, was generously provided by Dr. John Heider, formerly of Sandoz. (East Hanover, NJ) (25). A stock solution of 10 mg/ml was prepared in dimethyl sulfoxide and stored at −20 °C. All other chemical reagents were from Sigma.

Constructs and Antibodies—The cDNA encoding the human isoform of the SERCA2b in pcDNA 3.1(+) (19) was used for transient transfection. Goat anti-SERCA2 and anti-SERCA3 were from Santa Cruz Biotechnology, Inc. Rabbit anti-ribophorin-1 (26) and rabbit anti-Gos 28 (27) were generously provided by Dr. Gert Kreibich (New York University Medical Center) and Dr. Thomas Söllner (Memorial Sloane Kettering Research Institute), respectively. Rabbit anti-β_1-integrin was a gift of Dr. Eugene Marcantanio (Columbia University). Monoclonal anti-LAMP2 (ABL-93) was from the Developmental Hybridoma Bank (National Institutes of Health NICHHD, Iowa City, IA). Horseradish peroxidase-conjugated secondary antibodies were purchased from Jackson ImmunoResearch Laboratories.

Cell Culture—RAW 264.7 macrophages were cultured in RPMI 1640 supplemented with 10% heat-inactivated FBS and 100 units/ml penicillin/streptomycin. HEK293 cells were cultured in Dulbecco's modified Eagle's medium supplemented with 10% heat-inactivated fetal bovine serum (FBS) and 100 units/ml penicillin/streptomycin. Transient transfection of HEK293 cells with pcDNA3.1(+)-SERCA2b was achieved using LipofectAMINE® transfection reagent (Invitrogen) following the manufacturer's protocol, and the cells were studied 24 h after transfection. Mouse peritoneal macrophages were harvested from female wild-type C57BL6/J (Jackson Laboratories). Mice at 8–10 weeks of age were intraperitoneally injected with 0.5 ml of sterile phosphate-buffered saline (PBS) containing 40 μg of concanavalin A, and the macrophages were harvested 3 days later from the peritoneal lavage. The cells were cultured in Dulbecco's modified Eagle's medium supplemented with 10% FBS, 100 units/ml penicillin/streptomycin, and 20% L-cell-conditioned medium for 24–48 h to reach confluence. Macrophages were loaded with FC by incubation with acetyl-LDL (100 μg/ml) and compound 58035 (10 μg/ml) in Dulbecco's modified Eagle's medium supplemented with 1% FBS.

Methyl-β-cyclodextrin (MβCD)-Sterol Complex Preparation—50 μmol of MβCD was dissolved in 10 ml of Dulbecco's modified Eagle's medium, and 6.25 μmol of cholesterol, *ent*-cholesterol, or other sterol was added to this solution with vigorous vortexing. The dispersion was sonicated for 5 min at room temperature using a Fisher model 60 sonic dismembrator at setting 5. The solution was filtered through a 0.45-μm polyvinylidene difluoride membrane and kept in a glass tube under argon at 4 °C for up to a week. To determine the amount of sterol incorporated, the mixture was lipid extracted by the method of Bligh and Dyer (28) and then assayed for sterol content by gas chromatography using β-sitosterol as the standard (29).

Phospholipid Vesicle Preparation—A chloroform solution containing 3 μmol of phospholipid was dried under a nitrogen stream, and the dried lipids were then resuspended in 3 ml of PBS with vigorous vortexing. The dispersion was sonicated at 4 °C under argon using a Branson 450 sonicator with the duty cycle setting at 30% and the output setting at 4, until a clear solution was obtained. The solution was centrifuged for 1 h at 145,000 × *g* at 4 °C to remove any titanium particles and large multilamellar vesicles. The supernatant was filtered through a 0.45-μm polyvinylidene difluoride membrane and stored under argon.

Preparation of Microsomes—Cells on a 150-mm plate were rinsed twice with PBS and then detached by incubating with 2 ml of PBS, 2 mM EDTA for 5–10 min. The cells were pelleted by centrifugation at 500 × *g* for 5 min. The pellet was washed with PBS, re-centrifuged, resuspended into 2 ml of low-ionic strength buffer (10 mM Tris-HCl, pH 7.5, 0.5 mM $MgCl_2$, 1 mM phenylmethanesulfonyl fluoride, 100 units/ml aprotinin), and incubated on ice for 15 min. The cells were then homogenized with 40 strokes in a Dounce homogenizer with the type A pestle. Cell disruption was confirmed by trypan blue staining. The homogenate was made isotonic by the addition of 2 ml of 0.5 M sucrose, 0.3 M KCl, 6 mM β-mercaptoethanol, 40 μM $CaCl_2$, 10 mM Tris-HCl, pH 7.5, and then centrifuged at 8,000 × *g* for 20 min at 4 °C. The supernatant was transferred to a polycarbonate tube containing 0.9 ml of 2.5 M KCl, then centrifuged at 120,000 × *g* for 1 h at 4 °C. The pellet was washed twice and then resuspended in 200 μl of Buffer A (0.25 M sucrose, 0.15 M KCl, 3 mM β-mercaptoethanol, 20 μM $CaCl_2$, 10 mM Tris-HCl, pH 7.5). Protein concentration was measured by the Lowry assay using bovine serum albumin as the standard (30). The suspension was then snap frozen and stored in liquid nitrogen until use.

Endoplasmic Reticulum Membrane Fractionation—A sucrose step gradient was prepared by layering 3.0 ml of 1.1 M sucrose, 2.6 ml of 0.88 M sucrose, and 2.6 ml of 0.58 M sucrose in a 11-ml centrifuge tube, followed by refrigeration for 2 h at 4 °C. Cells from five 150-mm plates were collected and homogenized in 4 ml of low-ionic strength buffer as

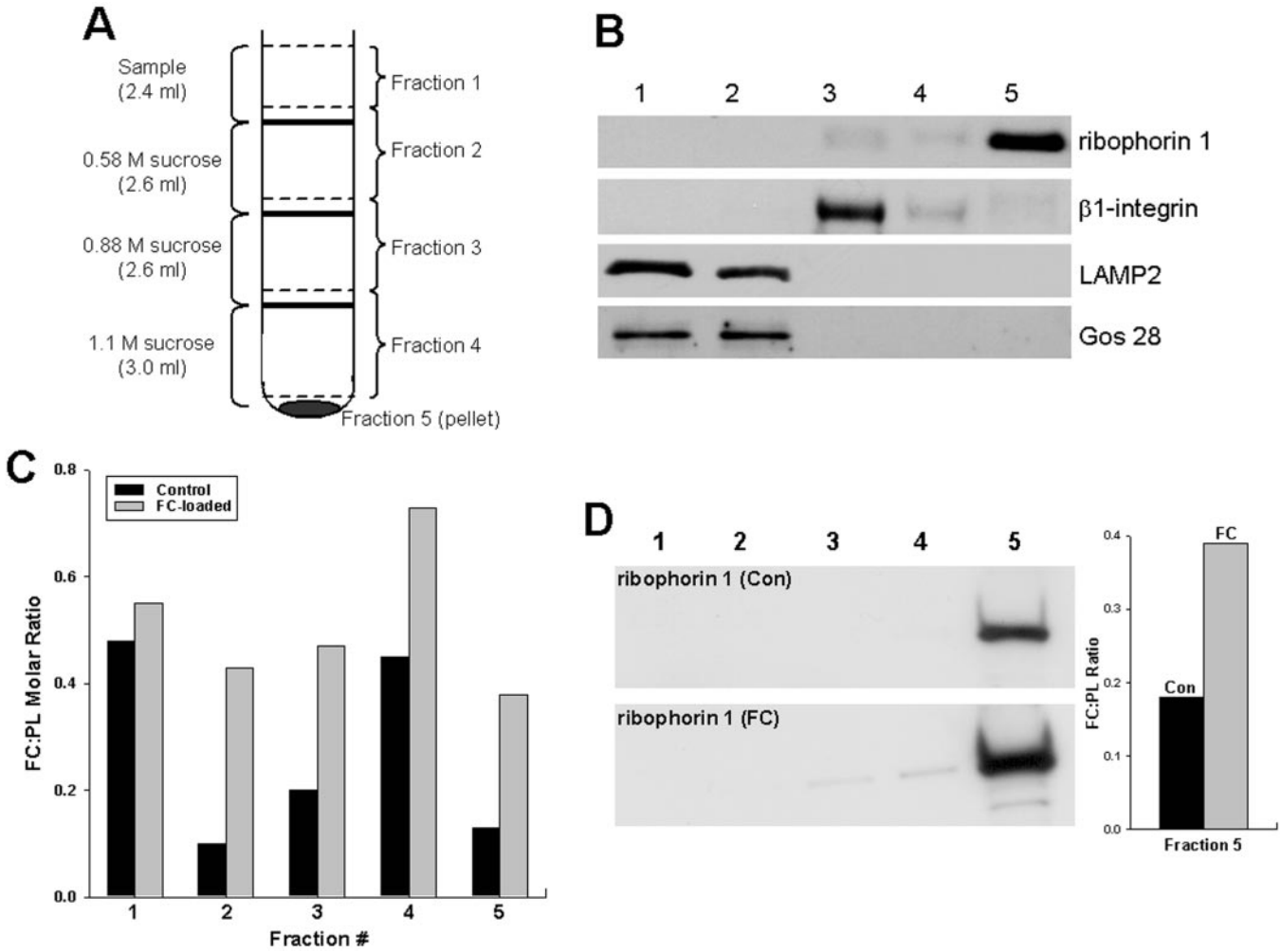

FIG. 1. **Cholesterol enrichment of ER-enriched membranes in FC-loaded macrophages.** Membranes from RAW and mouse peritoneal macrophages were fractionated by sucrose step-gradient centrifugation as described under "Experimental Procedures." *A*, fractionation scheme. The membranes at each interface are depicted by the *solid*, *bold lines*, and the boundaries of fractions 1–4 are depicted by the *dotted lines*. *B*, equal amounts of protein (50 μg) from each RAW macrophage fraction were subjected to SDS-PAGE and then immunoblotted for the ER marker ribophorin 1, the plasma membrane marker β_1-integrin, the Golgi marker Gos 28, and the late endosome/lysosome marker LAMP2. *C*, to assess cholesterol enrichment of ER *in vivo*, RAW macrophages were incubated in the absence or presence of 100 μg/ml acetyl-LDL and 10 μg/ml compound 58035 for 12 h. The membranes were fractionated as described in *A*, and lipid extracts from the five fractions were assayed for FC and phospholipid (*PL*) content. The experiment was repeated two additional times with similar results. *D*, fractions from mouse peritoneal macrophages were probed for ribophorin 1, and the fifth fraction was assayed for FC and phospholipid content.

described above. The homogenates were then made isotonic by the addition of 0.8 ml of low-ionic strength buffer containing 1.46 M sucrose and then centrifuged at 10,000 × *g* for 15 min at 4 °C. The supernatant (4.8 ml) was divided into two equal portions of 2.4 ml each, loaded onto two sucrose density gradient tubes, and centrifuged at 100,000 × *g* for 2 h at 4 °C. This procedure resulted in visible bands at each of the four interfaces plus a pellet. Five fractions were collected as depicted in Fig. 1*A*. The pellet, which was enriched in endoplasmic reticulum (see "Results"), was washed twice and then resuspended in 250 μl of Buffer A. Equal amounts of protein from each fraction were analyzed by SDS-PAGE and immunoblotting for organelle markers. Lipids from each fraction were extracted using the method of Bligh and Dyer (28) and analyzed for free cholesterol content by gas chromatography and for phospholipid content by the Bartlett assay (31).

Enrichment of Microsomal/ER Membranes with Sterols or Phospholipid in Vitro—Various amounts of sterols in complex with MβCD, or vesicles containing phospholipids with saturated or unsaturated fatty acids, were added to 100 μg of microsomal or endoplasmic reticulum membranes from HEK293T cells, and the final volume adjusted to 500 μl with Buffer A. After incubation at 25 °C for 30 min with gentle agitation, the samples were centrifuged at 120,000 × *g* for 1 h at 4 °C. The pellet was washed twice and then resuspended in Buffer A to a final concentration of 1 μg/μl for the assays described below.

Measurements of Ca^{2+}-dependent ATPase Activity—SERCA ATPase activity was measured using an enzyme-coupled spectrophotometric assay in which hydrolysis of ATP is coupled to the oxidation of NADH (32). The depletion of NADH was then detected by a decrease in absorption at 340 nm using a Spectra Max 190 fluorospectrometer (Molecular Devices) maintained at 30 °C. The assay buffer contained 120 mM KCl, 2 mM $MgCl_2$, 1 mM ATP, 1.5 mM phosphoenolpyruvate, 1 mM dithiothreitol, 0.45 mM $CaCl_2$, 0.5 mM EGTA, 25 mM MOPS/KOH, 0.32 mM NADH, 5 units/ml pyruvate kinase, 10 units/ml lactate dehydrogenase, and 2 μM of the calcium ionophore A23187. The pH was adjusted to 7.0 with KOH before addition of the enzymes, and the free Ca^{2+} concentration in the solution was determined to be ~3 μM. The reaction was started by adding 10 μg of the membranes to 200 μl of the assay buffer in wells of a 96-well UV-visible transparent bottom plate, followed by rapid mixing. The absorption at 340 nm was recorded at 30-s intervals for 30 min using the SOFTmax PRO 3.0 program.

Measurements of $^{45}Ca^{2+}$ Uptake into Membrane Vesicles—Ca^{2+} uptake activity was measured using an ATP-mediated oxalate-dependent assay (32). $^{45}CaCl_2$ was added to the uptake buffer (120 mM KCl, 25 mM MOPS/KOH, 3 mM $MgCl_2$, 0.45 mM $CaCl_2$, 0.5 mM EGTA, 5 mM potassium oxalate, 3 mM ATP, pH 7.0) to a final concentration of 1 μCi/ml. The reaction was started by adding 5 μg of membranes to 0.5 ml of Ca^{2+} uptake buffer in a clean glass tube at 25 °C with gentle mixing. At intervals of 5, 10, and 15 min, 150-μl aliquots were withdrawn from the reaction mixture and diluted into 3 ml of quench buffer (150 mM KCl, 1 mM $LaCl_3$) in a glass tube on ice. The buffer was filtered through a Millipore filtration manifold with a pre-wetted 0.3-μm PHWP nitrocellulose membrane, followed immediately by washing with 5 ml of cold quench buffer. The membrane was removed from the manifold, and

radioactivity was measured by a liquid scintillation counter.

ESR Spectroscopy and Non-linear Least Squares Fitting of ESR Spectra—5 μl of 0.28 mM 16-doxyl-PC in methanol was added to 250 μl of PBS containing 250 μg of control or FC-enriched ER membranes. The labeled dispersion was vortexed for 30 s, then diluted with PBS to 4 ml and centrifuged at 120,000 × *g* for 1 h at 4 °C. The pellet was transferred to a quartz capillary tube for ESR measurements. ESR spectra were obtained using a Bruker Instruments (Billerica, MA) EMX ESR spectrometer at a frequency of 9.34 GHz equipped with a Varian temperature controller. The non-linear least squares analyses of the spectra were performed using the latest version of the ESR fitting program (33). These analyses yield the following parameters: rotational diffusion rate $R_\perp$ and order parameters S_0, S_2. $R_\perp$ is the rotational rate of the nitroxide radical around an axis perpendicular to the mean symmetry axis for the rotation. This symmetry axis is also the direction of preferential orientation of the spin-labeled molecule (34). The order parameter S_0 is a measure of the angular extent of the rotational diffusion of the nitroxide moiety relative to the membrane director (the normal to the lipid bilayer). The larger the S_0, the more restricted is the motion, which usually means that laterally the lipid molecules surrounding the nitroxide radical are packed more tightly. S_2 is the non-symmetric order parameter, which represents the nonaxiality of the preferential orientation of the spin-labeled molecule relative to the membrane director. Thus, for S_2, the restriction of the wagging motion of the spin label is not symmetric about its main symmetry axis.

RESULTS

Cholesterol Accumulation in ER-enriched Membranes from FC-loaded Macrophages—FC trafficking to the ER is a necessary step in ER calcium depletion in FC-loaded macrophages (9). As a prelude to our study on the effects of increased ER cholesterol on SERCA activity, we determined the level of cholesterol accumulation in the ER in FC-loaded macrophages. For this purpose, we developed a sucrose density step-gradient fractionation procedure for the isolation of an ER-enriched fraction in RAW and mouse peritoneal macrophages (Fig. 1*A*). As shown in Fig. 1*B* for RAW macrophages and Fig. 1*D* for mouse peritoneal macrophages, the fifth fraction (pellet) was enriched in the ER-specific protein ribophorin (26). The blot in Fig. 1*B* shows no detectable LAMP2 (lysosomes), Gos 28 (Golgi), or β_1-integrin (plasma membrane) in fraction 5. As expected for an ER-enriched fraction (35), the FC:phospholipid ratio of fraction 5 was relatively low (*black bars* in Fig. 1, *C* and *D*). With FC loading of the macrophages, the FC:phospholipid ratio of the ER-enriched fraction increased ~2–2.5-fold (*gray bars* in Fig. 1, *C* and *D*).

SERCA Expression in Control and FC-loaded Macrophages—In theory, ER calcium depletion in FC-loaded macrophages could be caused by activation of calcium release channels and/or inhibition of SERCA. Initial experiments with inositol 1,4,5-trisphosphate receptor and the ryanodine receptor intracellular calcium release channels reconstituted in planar lipid bilayer membranes with different FC:phospholipid ratios revealed no evidence of consistent cholesterol-induced activation of these channels (data not shown). We therefore focused on the hypothesis that cholesterol inhibits SERCA. In this context, we first determined which isoform(s) of SERCA were expressed in macrophages. As shown by the immunoblot in Fig. 2*A* (*first two lanes*), RAW macrophages and mouse peritoneal macrophages express SERCA2b; SERCA1 and -3 could not be detected (not displayed). Previous studies by Caspersen *et al.* (36) showed that SERCA2b expression in PC12 cells was increased by inducers of the UPR. Because FC loading induces the UPR in macrophages (9), we assayed SERCA2b protein levels in control and FC-loaded macrophages. As shown in Fig. 2*B*, FC loading led to an ~2-fold increase in SERCA2b expression that preceded maximum induction of the UPR effector CHOP.

As expected, SERCA2b activity in microsomes isolated from macrophages was too low to be measured *in vitro*. Because macrophages are very difficult to transfect, we used SERCA2b-transfected HEK293 cells as the source of SERCA2b-containing membranes for our study. As shown in Fig. 2*A* (*third lane*), endogenous SERCA2b was undetectable in HEK293 cells, whereas 24 h after transient transfection, the cells expressed abundant SERCA2b (fourth lane in Fig. 2*A*; note that 10 μg of protein was loaded in the *fourth lane versus* 50 μg for the *first three lanes*). Immunostaining of the transfected cells showed that SERCA2b was expressed in a distinct ER pattern (not shown).

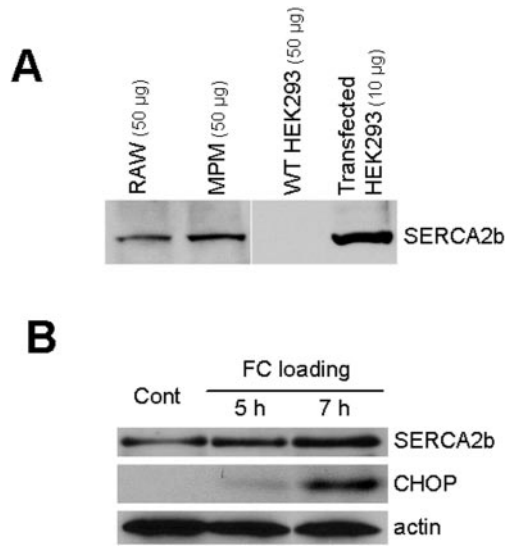

FIG. 2. **SERCA expression in macrophages and transfected HEK293 cells.** *A*, cell lysates from mouse peritoneal macrophages (50 μg), RAW macrophages (50 μg), wild-type HEK293 (50 μg), or SERCA2b-overexpressing HEK293 (10 μg) were subjected to SDS-PAGE and immunoblot analysis for SERCA2b. *B*, cell lysates (50 μg) from control mouse peritoneal macrophages and macrophages loaded with FC for 5 or 7 h were subjected to SDS-PAGE and immunoblot analysis for SERCA2b, CHOP, and actin. Repeat experiments yielded similar results.

Cholesterol Enrichment Inhibits SERCA2b Activity—To determine the effects of membrane cholesterol enrichment on SERCA2b activity *in vitro*, we incubated SERCA2b-containing microsomes with various amounts of cholesterol in complex with MβCD. The microsomes were then recovered by centrifugation, and SERCA2b activity was measured. Cholesterol enrichment of the microsomes inhibited both SERCA2b calcium ATPase activity (Fig. 3*A*) and SERCA2b-mediated $^{45}Ca^{2+}$ uptake (Fig. 3*B*) in the same dose-dependent manner, with a 50% inhibition of both when incubated with 1.5 μg of cholesterol. Incubation with MβCD alone did not affect SERCA2b activity (*inset* in Fig. 3*A*). The inhibition of these processes by the specific SERCA inhibitor thapsigargin confirmed that these measurements represented SERCA activity.

To determine the increase in the FC:phospholipid molar ratio that is associated with inhibition of SERCA2b ATPase activity, we repeated the experiment described above using ER-enriched membranes from the SERCA2b-transfected HEK293 cells. Using a concentration of MβCD-cholesterol that inhibited SERCA2b ATPase activity by ~50% (Fig. 4*A*), the FC:phospholipid molar ratio of the membranes was increased by ~2-fold (Fig. 4*B*). As demonstrated by the data for fraction 5 in Fig. 1*C*, this is very similar to the increase in the FC:phospholipid molar ratio that occurs in the ER in FC-loaded macrophages.

Comparison of the Effect of Nat-Cholesterol, Ent-Cholesterol, and Epi-Cholesterol on SERCA Activity—There are two major mechanisms that could explain FC-induced SERCA2b inhibition, namely, alteration of ER membrane structure or direct

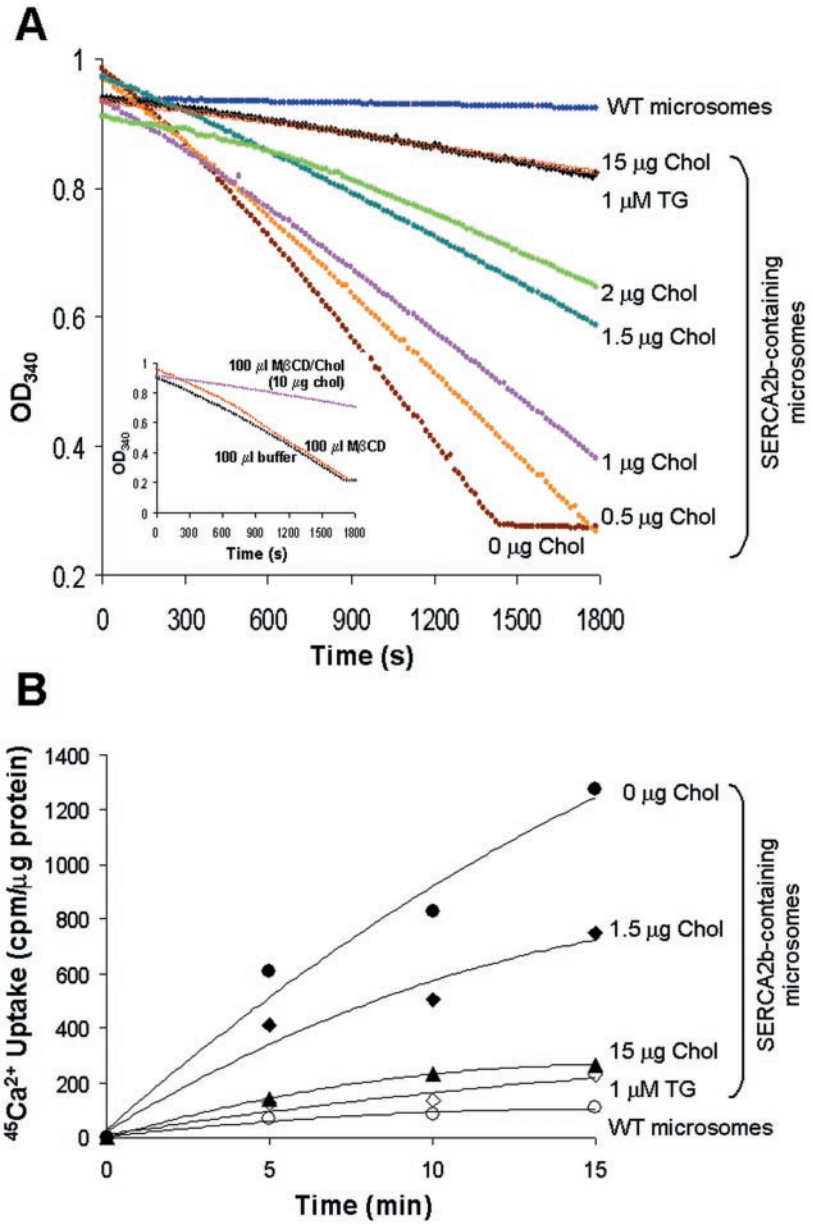

FIG. 3. **Cholesterol enrichment of SERCA2b-containing microsomes inhibits SERCA2b activity.** 100 μg of microsomal membranes from SERCA2b-transfected HEK293 cells were incubated with various amounts of cholesterol (*Chol*) complexed with MβCD for 30 min. The membranes were re-isolated by centrifugation and assayed for SERCA2b activity. *A*, Ca^{2+}-ATPase activity, as measured by a decrease in absorption at 340 nm, indicative of consumption of NADH in this enzyme-coupled assay. The *inset* shows that incubation of microsomes with MβCD alone does not inhibit SERC2b activity. *B*, microsomal $^{45}Ca^{2+}$ uptake activity. Negative controls included membranes from SERCA2b-transfected HEK293 cells treated with 1 μM thapsigargin (*TG*) or re-suspended in a Ca^{2+}-free buffer (not displayed) and membranes from non-transfected HEK293 cells. Both experiments were repeated three times with similar results.

binding of cholesterol to SERCA2b or a SERCA2b-regulatory protein. To distinguish between these two mechanisms, we first compared the effect of *nat*-cholesterol and *ent*-cholesterol on SERCA2b activity. *Nat*-Cholesterol and its enantiomer, *ent*-cholesterol, have identical effects on membrane properties such as enhancement of membrane order, interaction with phospholipids, and promotion of membrane rafts (22). In contrast, cholesterol and *ent*-cholesterol interact differently with cholesterol-binding proteins such as cholesterol oxidase or *Vibrio* cytolysin (37). We therefore incubated SERCA2b-containing ER membranes with MβCD complexed with either *nat*- or *ent*-cholesterol and then assayed the membranes for the sterol:phospholipid ratio and SERCA2b ATPase activity. Similar amounts of *nat*- and *ent*-cholesterol were incorporated into the membranes, and SERCA2b ATPase activity was inhibited to the same extent (~60%) by the two sterols (Fig. 5*A*). On the other hand, when a similar amount of 3-e*pi*-cholesterol was incorporated into the membranes, the SERCA2b ATPase activity was not affected (Fig. 5*B*), which is consistent with previous studies showing that the 3-epimer of cholesterol orders membrane lipids to a much lesser extent than cholesterol (21, 38). These data are most consistent with a model in which FC-induced changes in ER membrane structure is the cause of SERCA2b inhibition.

Manipulation of Phospholipid Composition—Cholesterol enrichment of biological membranes increases the order, or "stiffness," of those membranes (39, 40). If this were the mechanism behind FC-induced inhibition of SERCA2b activity, we should be able to inhibit SERCA2b by other perturbations that increase membrane order. Other investigators have shown that the order of biological membranes containing unsaturated fatty acid-containing PC can be increased *in vitro* by replacing endogenous PC with PC containing saturated fatty acids (41). We therefore incubated SERCA2b-containing membranes with small unilamellar vesicles made from 14:0–18:0 PC or 18:1–18:1 PC, re-isolated the membranes, and then assayed SERCA2b ATPase activity. As shown in Fig. 6, membranes that had been incubated with 14:0–18:0 PC had much less SERCA2b activity than those incubated with 18:1–18:1 PC. These data further support the concept that SERCA2b activity is compromised when the membrane order is increased.

Direct Evaluation of Membrane Fluidity by Electron Spin Resonance—To further evaluate the hypothesis that FC-induced SERCA2b inhibition was related to the membrane or-

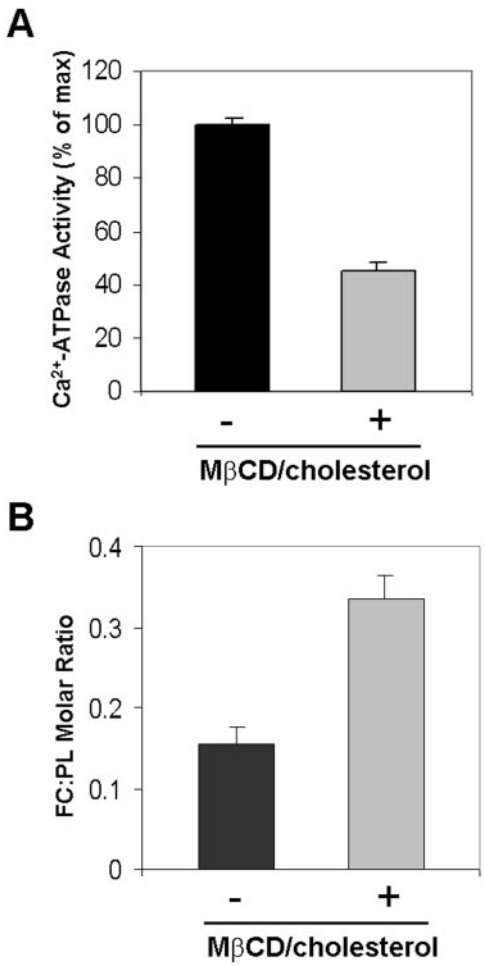

FIG. 4. **Extent of ER cholesterol accumulation at 50% inhibition of SERCA2b activity.** 500 μg of ER-enriched membranes from SERCA2b-overexpressing HEK293 cells were incubated with 7.5 μg of cholesterol in complex with MβCD and then re-isolated by centrifugation. The Ca^{2+}-ATPase activity of SERCA2b (*A*) and the contents of FC and phospholipid (*PL*) (*B*) in the control and FC-loaded membranes were measured. For both experiments, $n = 3$ measurements from a single experiment, ±S.E. Similar results were obtained from two repeat experiments.

dering effects of cholesterol, we sought to determine directly the relationship between the FC:phospholipid ratio, membrane order, and SERCA2b activity. To achieve this goal, ER-enriched membranes from SERCA2b-transfected HEK293 cells were incubated in the absence or presence of MβCD-cholesterol, and separate aliquots were taken for assays of lipid mass, SERCA2b ATPase activity, and membrane order using electron spin resonance (ESR). For the ESR studies, the 16-doxyl-PC spin label probe was added to the membranes, and ESR spectra were obtained at 22 and 37 °C (Fig. 7*A*). The *black lines* in this figure (shown for the 37 °C spectra) represent the experimental data, and the *red lines* are the least-squares fits of these data. All the spectra are fitted with two components, one of which is a spectrum with the normal three hyperfine lines, and the other is a single broad line. For illustration, the two components for the spectrum at 37 °C containing 32 mol % cholesterol are shown in Fig. 7*B*.

The best fit values of $R_\perp$, S_0, and S_2 for the first component at both 22 and 37 °C for each of the three membrane samples are listed in Table I, along with the FC:phospholipid molar ratio. The broad component in the spectra is a clear indication of strong spin-spin interactions that would be expected from clustering of some of the 16-doxyl-PC molecules in the sample (42). As shown in Table I, the amounts of the broad component are not greatly different in membranes loaded with different amounts of cholesterol, and this broad component does not provide information about the motional characteristics of the ER bilayer. Therefore, we restricted our analysis to the first component, which exhibits hyperfine lines. Using the 37 °C data, we plotted $R_\perp$, S_0, and percent inhibition of SERCA2b ATPase activity as a function of the FC:phospholipid ratio in the membranes (Fig. 7*C*). The data show a striking correlation among these three parameters, which is consistent with the aforementioned model in which cholesterol-induced ordering of the normally fluid ER membrane inhibits SERCA2b function.

DISCUSSION

Cholesterol and related sterols are an essential component of membrane lipid bilayers in eukaryotic cells (43). Sterols have important effects on the physical properties of biological membranes, and these effects, in turn, can influence the structure and function of integral membrane proteins (44). Most notably, cholesterol increases phospholipid ordering and widens the bilayer by reducing the number of phospholipid molecules in the *gauche* conformation (45). In normal physiology, cholesterol-induced lipid ordering in membrane microdomains ("rafts") regulates a number of essential protein-protein interactions, such as those involved in signal transduction (46). However, studies *in vitro* have shown that excessive ordering of membrane lipids by the introduction of superphysiologic amounts of cholesterol can perturb protein function. Several mechanisms that might account for loss of membrane protein function under these conditions are a decrease in the conformational "freedom" of proteins, induction of dysfunctional protein "aggregation," an increase in bilayer thickness, and separation of lipid phases (40, 45, 47, 48).

Whereas these *in vitro* studies examining effects of excess cholesterol on protein function have established important theoretical principles, they have generally not been connected with specific pathophysiological processes. The present study was conceived in the context of a critical cell biological event occurring in advanced atherosclerosis, namely accumulation of excess FC by macrophages. *In vivo* data suggest that a portion of this FC overloads the ER membrane (9, 12), and cell culture data have shown that depletion of ER calcium stores is an important consequence that can be directly attributable to ER cholesterol overload (9). Because excess membrane cholesterol does not appear to activate ER calcium release channels, we hypothesized that inhibition of SERCA2b, the form of SERCA in macrophages, was the primary cause of loss of ER calcium. In the context of these *in vivo* findings, we show here that enrichment of ER *in vitro* with a level of cholesterol that occurs *in vivo* in FC-loaded macrophages does indeed inhibit the activity of SERCA2b.

The inhibition of SERCA2b activity by *ent*-cholesterol and by phospholipids containing saturated fatty acids suggested that the mechanism was because of increased ordering of the ER membrane rather than a direct interaction with cholesterol *per se*. To directly examine changes in the biophysical characteristics of ER membranes as cholesterol loading is increased, we used ESR spectral analysis of 16-doxyl-PC incorporated into ER membranes. As shown in Table I, the $R_\perp$ and S_0 of the ER membrane with no added cholesterol (FC:phospholipid molar ratio = 0.12) are similar to those of liquid-disordered membranes, which is consistent with previous studies of the properties of ER membranes (21). As the cholesterol content is increased to a FC:phospholipid molar ratio of 0.33, the order parameter S_0 increases significantly. The S_0 of 16-doxyl-PC in ER membranes loaded with these high levels of cholesterol is close to the S_0 of 16-doxyl-PC in the liquid-ordered phase of lipid bilayers consist-

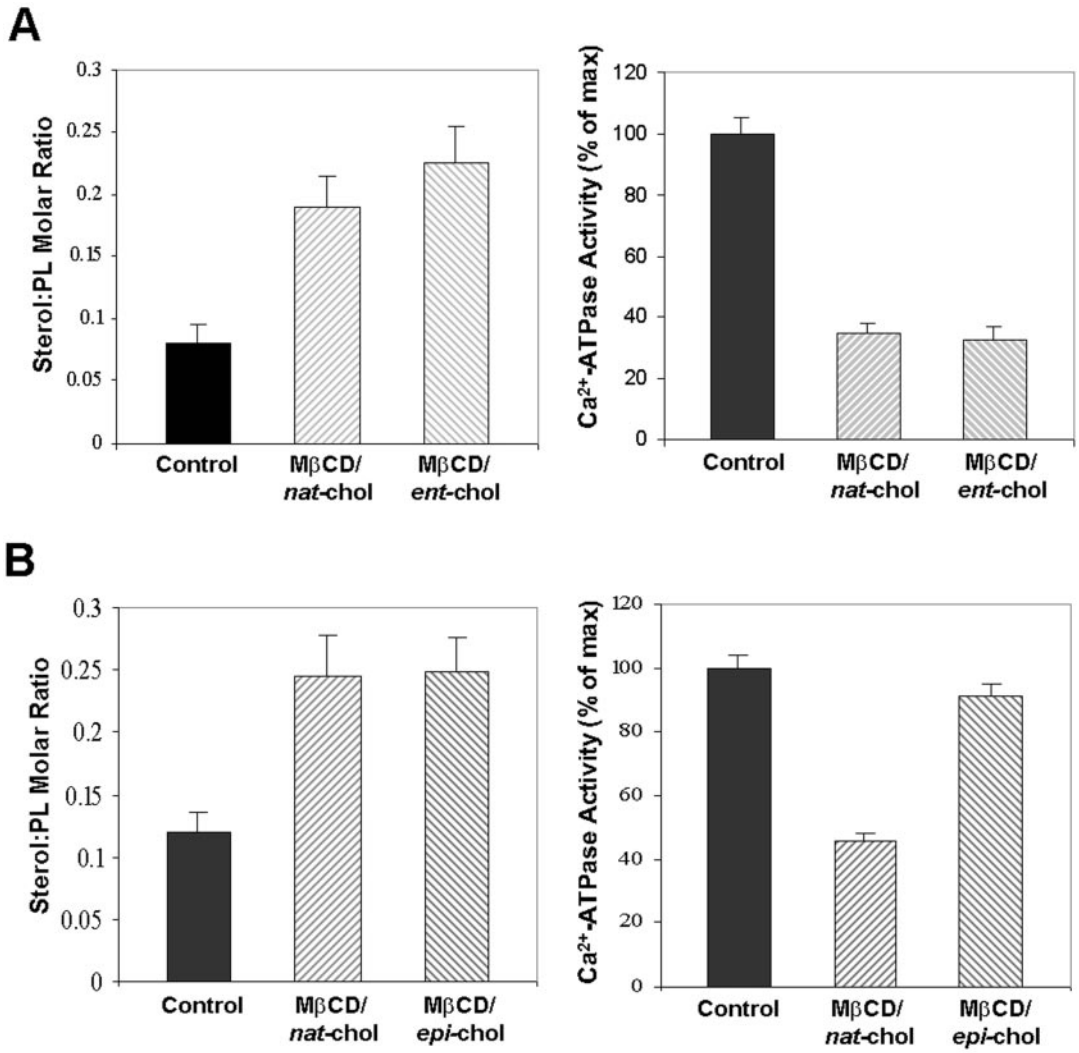

FIG. 5. **Effect of *ent*-cholesterol and *epi*-cholesterol enrichment of SERCA2b-containing microsomes on SERCA2b activity.** 500 μg of ER-enriched membranes from SERCA2b-transfected HEK293 cells were incubated with 7.5 μg of *nat*-cholesterol (*Chol*) (*A* and *B*), *ent*-cholesterol (*A*), or *epi*-cholesterol (*B*) in complex with MβCD and then re-isolated by centrifugation. Sterol and phospholipid (*PL*) mass and Ca^{2+}-ATPase activity of these samples were measured. For both experiments, $n = 3$ measurements from a single experiment, $\pm$S.E. Similar results were obtained from two repeat experiments.

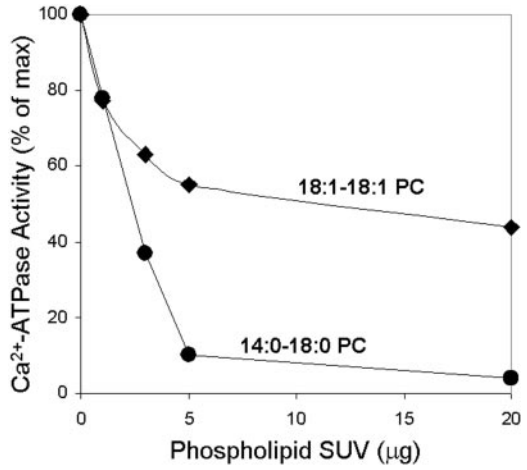

FIG. 6. **Incubation of SERCA2b-containing microsomes with saturated phospholipids inhibits SERCA2b activity.** 100 μg of microsomal membranes from SERCA2b-transfected HEK293 cells were incubated with various amounts of PC vesicles consisting of 14:0–18:0 PC (*circles*) or 18:1–18:1 PC (*diamonds*). The membranes were re-isolated by centrifugation and then assayed for Ca^{2+}-ATPase activity. Each point represents duplicate measurements, which varied by <5%. *SUV*, small unilamellar vesicles.

ing of dipalmitoyl phosphatidylcholine (DPPC) and cholesterol at a molar ratio of 1:1, which is 0.22 at 25–35 °C (49). The S_0 values are also similar to those obtained in detergent-resistant membranes from rat basophilic leukemia (RBL) cells, which is 0.20 at 37 °C (49). These changes in the order parameter indicate that the ER membrane undergoes a significant extent of ordering with FC enrichment, with its properties becoming similar to liquid-ordered membranes. The $R_\perp$ values change less dramatically as cholesterol is increased, with values that are also consistent with a liquid-ordered membrane organization.

In considering these data, it is important to note that the ER membrane normally has a relatively low FC:phospholipid ratio and saturated fatty acid content and is therefore one of the most fluid membranes in the cell (21, 35). Indeed, a recent report showed that the ER membrane, unlike the plasma membrane, is actually permeable to small charged molecules, which is a property of low-order membranes (50). Thus, one would expect that a number of integral membrane proteins in the ER are adapted to function optimally in this fluid membrane environment and would therefore be adversely affected by an increase in membrane order. In this regard, SERCA contains multiple transmembrane domains, and its calcium pumping cycle requires several changes in protein conformation (51, 52).

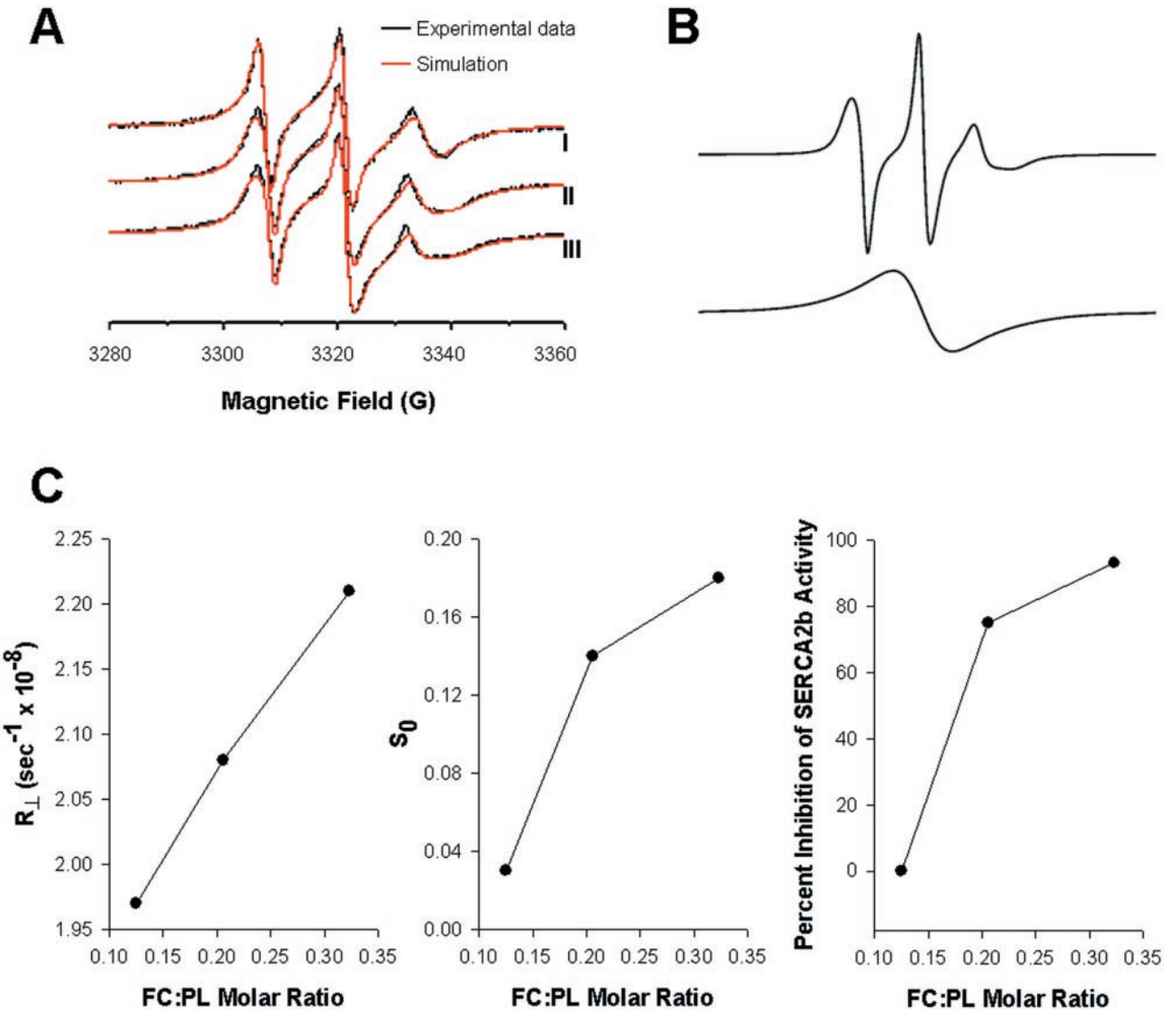

FIG. 7. **ESR spectroscopy of 16-doxyl-PC-labeled control or FC-loaded ER-enriched membranes.** 500 μg of ER membranes from SERCA2b-transfected HEK293 cells were incubated with buffer (*sample I*) or with various amounts of cholesterol (*sample II*: 10 μg; *sample III*: 20 μg) in complex with MβCD. After re-isolation by centrifugation, half of the membranes were mixed with 16-doxyl-PC spin label and subjected to ESR spectroscopy, and the other half were assayed for content of FC and phospholipids. *A*, ESR spectra (*black line*) and the non-linear least-square fitting (*red line*) of 16-doxyl-PC in the ER membranes. *B*, two components for the spectrum of 16-doxyl-PC at 37 °C in sample III. The fractional population (*P*) of the first spectral component (top tracing) range from 0.23 to 0.29. *C*, rotational diffusional rate ($R_\perp$), order parameter (S_0), and percent inhibition of SERCA2b ATPase activity as a function of the FC:PL ratio in the ER membranes. A repeat experiment yielded similar results. See Table I for additional ESR measurements.

TABLE I

Parameters obtained from nonlinear least-squares fitting of ESR spectra of 16-doxyl-PC in ER-enriched membranes (component 1) at 22 and 37 °C

ER-enriched membranes from SERCA2b-transfected HEK293 cells were used in their natural state (Sample I) or loaded with increasing concentrations of FC (Samples II and II). After addition of 16-doxyl-PC, ESR spectra were obtained at 22 and 37 °C. The magnetic parameters used in the simulations are: g_{xx}, g_{yy}, and g_{zz} = 2.0082, 2.0064, and 2.0020; A_{xx}, A_{yy}, and A_{zz} (G) = 5.0, 5.0, and 33.5 G. The estimated errors were ±5% for $R_\perp$ and ±0.02 for S_0 and S_2. $R_\perp$, S_0, and S_2, are defined under "Experimental Procedures."

Sample	FC:PL[a]	T	$R_\perp$	S_0	S_2
		°C	s^{-1}		
I	0.12	22	1.50×10^8	0.04	−0.12
		37	1.97×10^8	0.03	−0.11
II	0.21	22	1.97×10^8	0.17	−0.22
		37	2.08×10^8	0.14	−0.22
III	0.32	22	1.82×10^8	0.19	−0.24
		37	2.21×10^8	0.18	−0.28

[a] FC:PL, FC:phospholipid molar ratio.

Restriction of these conformation changes in a more ordered membrane is a plausible mechanism accounting for the decrease in SERCA activity in cholesterol-enriched ER. This hypothesis is consistent with the frequency domain phosphorescence spectroscopy data of Hunter *et al.* (53) and Whiting *et al.* (54), and with the saturation-transfer electron paramagnetic resonance data of Squier *et al.* (55). While separation of lipid phases is an additional mechanism that might account for SERCA inhibition, we did not find evidence for this phenomenon in ER membranes as the cholesterol level was changed. Nonetheless, this negative result does not rule out the possibility that such domain formation occurs.

Previous studies have explored the effect of cholesterol enrichment of membranes and vesicles containing SERCA1 from the sarcoplasmic reticulum of skeletal muscle, although there have been potential methodological problems and, in some cases, contradictory results. All of these studies used DPPC-cholesterol vesicles to enrich membranes with cholesterol, often without re-isolating the membranes. As shown by the data

of Fig. 6 in the current study, DPPC itself would likely influence SERCA activity. In one of these studies, DPPC-cholesterol was found to inhibit SERCA1 activity (56), but in another study this result was not obtained, and the authors attributed the previous finding to an artifact related to the absence of dithiothreitol in the incubation mixture (57). Moreover, neither of these studies reported membrane fluidity measurements. In a more recent study, both DPPC-cholesterol and progesterone enrichment of SERCA1-containing membranes increased membrane order as measured by fluorescence polarization, but only cholesterol inhibited SERCA1 activity (54). Cheng *et al.* (58) reconstituted SERCA1 in synthetic vesicles containing PC, phosphatidylethanolamine, and cholesterol. Vesicles with a high cholesterol:phospholipid ratio demonstrated decreased fluidity and decreased ATPase activity, but calcium uptake was either not affected or actually increased, depending on the relative amounts of phosphatidylcholine and phosphatidylethanolamine. Overall, these studies tend to support the idea that skeletal muscle SERCA1 ATPase is adversely affected by cholesterol-induced membrane stiffening, which is consistent with the SERCA2b data in this report, but the caveats and inconsistencies outlined above are notable. Moreover, a physiologic or pathophysiologic context in which the cholesterol content of muscle sarcoplasmic reticulum might be increased has not been demonstrated.

Of interest, two other ER membrane proteins involved in intracellular cholesterol metabolism appear to be affected more by direct cholesterol-protein interactions than by cholesterol-induced changes in membrane fluidity. Cholesterol-mediated regulation of the sterol regulatory element-binding protein pathway involves a conformational change in sterol regulatory element-binding protein cleavage-activating protein (SCAP). In this scenario, sterol specificity data are consistent with a direct sterol-SCAP interaction causing this effect (59, 60). Indeed, SCAP contains a consensus "sterol-sensing domain" that likely mediates this interaction (44), although direct sterol binding to this protein has not yet been demonstrated. In another scenario, Chang and colleagues (61) have shown that a number of sterols activate ACAT by a mechanism thought to involve an allosteric sterol-enzyme interaction, although ACAT may actually be suppressed when the order of the ER membrane is increased by other lipids (62).

As mentioned above, FC loading of cultured macrophages leads to ER calcium depletion, UPR induction, and apoptosis, all of which are completely dependent on FC trafficking to the ER (9, 12). Depletion of ER calcium stores is a known inducer of the UPR (13, 14), and we have shown that the UPR is necessary for FC-induced apoptosis. Thus, ER calcium depletion, which is an early event in macrophage FC loading, could be a key upstream event leading to macrophage death. Interestingly, Rodriguez and colleagues (63) have reported that macrophage-like cells derived from cultured human blood monocytes do not accumulate large amounts of FC and therefore, as expected, do not die when incubated with acetyl-LDL and an ACAT inhibitor. This finding is associated with a high level of cholesterol efflux and down-regulation of the scavenger receptor. However, there is evidence that human and murine lesional macrophages behave more similarly to the primary macrophages used in the current study. For example, advanced lesional macrophages are known to be FC-loaded (7), and we have shown that they express the UPR effector CHOP (9). Moreover, a genetic manipulation that blocks FC trafficking to the ER *in vivo* protected lesional macrophage from apoptotic death (12).

If ER calcium depletion is an important inducer of these events, then inhibition of SERCA2b by cholesterol-induced ordering of the normally fluid ER membrane might represent a biophysical explanation of why arterial wall cholesterol is associated with advanced atherothrombotic disease. On a broader scale, the findings in this report would imply that other integral membrane proteins in the ER, particularly those with multiple membrane-spanning regions and those whose mechanism involves changes in protein conformation, might also be adversely affected in advanced, FC-loaded lesional macrophages. Indeed, recent work has shown that cholesterol enrichment of ER membranes *in vitro* can inhibit the translocation of newly synthesized proteins (64). The testing of these ideas must await the development of new strategies in which calcium depletion in particular and ER membrane fluidity changes in general could be prevented in FC-loaded macrophages. Such strategies might also form the basis of novel therapeutic approaches to the problem of the unstable atherosclerotic plaque.

Acknowledgments—We thank Dr. Andrew Marks for helpful discussions and advice related to ER calcium channels, Dr. Rebecca Juliano for assistance with the ESR studies, and Inge Hansen for the GC analysis.

REFERENCES

1. Ross, R. (1995) *Annu. Rev. Physiol.* **57,** 791–804
2. Libby, P., and Clinton, S. K. (1993) *Curr. Opin. Lipidol.* **4,** 355–363
3. Brown, M. S., and Goldstein, J. L. (1983) *Annu. Rev. Biochem.* **52,** 223–261
4. Chang, T. Y., Chang, C. C., Lin, S., Yu, C., Li, B. L., and Miyazaki, A. (2001) *Curr. Opin. Lipidol.* **12,** 289–296
5. Rapp, J. H., Connor, W. E., Lin, D. S., Inahara, T., and Porter, J. M. (1983) *J. Lipid Res.* **24,** 1329–1335
6. Small, D. M., Bond, M. G., Waugh, D., Prack, M., and Sawyer, J. K. (1984) *J. Clin. Investig.* **73,** 1590–1605
7. Tabas, I. (2002) *J. Clin. Investig.* **110,** 905–911
8. Mallat, Z., Hugel, B., Ohan, J., Leseche, G., Freyssinet, J. M., and Tedgui, A. (1999) *Circulation* **99,** 348–353
9. Feng, B., Yao, P. M., Li, Y., Devlin, C. M., Zhang, D., Harding, H. P., Sweeney, M., Rong, J. X., Kuriakose, G., Fisher, E. A., Marks, A. R., Ron, D., and Tabas, I. (2003) *Nat. Cell Biol.* **5,** 781–792
10. Zinszner, H., Kuroda, M., Wang, X., Batchvarova, N., Lightfoot, R. T., Remotti, H., Stevens, J. L., and Ron, D. (1998) *Genes Dev.* **12,** 982–995
11. Oyadomari, S., Koizumi, A., Takeda, K., Gotoh, T., Akira, S., Araki, E., and Mori, M. (2002) *J. Clin. Investig.* **109,** 525–532
12. Feng, B., Zhang, D., Kuriakose, G., Devlin, C. M., Kockx, M., and Tabas, I. (2003) *Proc. Natl. Acad. Sci. U. S. A.* **100,** 10423–10428
13. Brostrom, C. O., and Brostrom, M. A. (1998) *Prog. Nucleic Acids Res. Mol. Biol.* **58,** 79–125
14. Bertolotti, A., Zhang, Y., Hendershot, L. M., Harding, H. P., and Ron, D. (2000) *Nat. Cell Biol.* **2,** 326–332
15. East, J. M. (2000) *Mol. Membr. Biol.* **17,** 189–200
16. Brandl, C. J., deLeon, S., Martin, D. R., and MacLennan, D. H. (1987) *J. Biol. Chem.* **262,** 3768–3774
17. Lytton, J., and MacLennan, D. H. (1988) *J. Biol. Chem.* **263,** 15024–15031
18. Burk, S. E., Lytton, J., MacLennan, D. H., and Shull, G. E. (1989) *J. Biol. Chem.* **264,** 18561–18568
19. Lytton, J., Westlin, M., Burk, S. E., Shull, G. E., and MacLennan, D. H. (1992) *J. Biol. Chem.* **267,** 14483–14489
20. Wu, K. D., Lee, W. S., Wey, J., Bungard, D., and Lytton, J. (1995) *Am. J. Physiol.* **269,** C775–C784
21. Davis, P. J., and Poznansky, M. J. (1987) *Proc. Natl. Acad. Sci. U. S. A.* **84,** 118–121
22. Westover, E. J., Covey, D. F., Brockman, H. L., Brown, R. E., and Pike, L. J. (2003) *J. Biol. Chem.* **278,** 51125–51133
23. Havel, R. J., Eder, H., and Bragdon, J. (1955) *J. Clin. Investig.* **34,** 1345–1353
24. Basu, S. K., Goldstein, J. L., Anderson, G. W., and Brown, M. S. (1976) *Proc. Natl. Acad. Sci. U. S. A.* **73,** 3178–3182
25. Ross, A. C., Go, K. J., Heider, J. G., and Rothblat, G. H. (1984) *J. Biol. Chem.* **259,** 815–819
26. Marcantonio, E. E., Grebenau, R. C., Sabatini, D. D., and Kreibich, G. (1982) *Eur. J. Biochem.* **124,** 217–222
27. Nagahama, M., Orci, L., Ravazzola, M., Amherdt, M., Lacomis, L., Tempst, P., Rothman, J. E., and Sollner, T. H. (1996) *J. Cell Biol.* **133,** 507–516
28. Bligh, E. G., and Dyer, W. J. (1959) *Can. J. Biochem. Physiol.* **37,** 911–917
29. Ishikawa, T. T., MacGee, J., Morrison, J. A., and Glueck, C. J. (1974) *J. Lipid Res.* **15,** 286–291
30. Lowry, O. H., Rosebrough, N. J., Farr, A. L., and Randall, R. J. (1951) *J. Biol. Chem.* **193,** 265–275
31. Bartlett, G. R. (1959) *J. Biol. Chem.* **234,** 466–468
32. Lytton, J., Westlin, M., and Hanley, M. R. (1991) *J. Biol. Chem.* **266,** 17067–17071
33. Budil, D. E., Lee, S., Saxena, S., and Freed, J. H. (1996) *J. Magn. Reson. A* **120,** 155–189 (abstr.)
34. Schneider, D. J., and Freed, J. H. (1989) *Spin Label Theory and Applications*, Plenum Press, New York
35. Lange, Y., and Steck, T. L. (1997) *J. Biol. Chem.* **272,** 13103–13108
36. Caspersen, C., Pedersen, P. S., and Treiman, M. (2000) *J. Biol. Chem.* **275,** 22363–22372

37. Zitzer, A., Westover, E. J., Covey, D. F., and Palmer, M. (2003) *FEBS Lett.* **553,** 229–231
38. Rog, T., and Pasenkiewicz-Gierula, M. (2003) *Biophys. J.* **84,** 1818–1826
39. Yeagle, P. L. (1985) *Biochim. Biophys. Acta* **822,** 267–287
40. Yeagle, P. L. (1991) *Biochimie* (*Paris*) **73,** 1303–1310
41. Dolis, D., de Kroon, A. I., and de Kruijff, B. (1996) *J. Biol. Chem.* **271,** 11879–11883
42. Fajer, P., Watts, A., and Marsh, D. (1992) *Biophys. J.* **61,** 879–891
43. Brown, D. A., and London, E. (1998) *J. Membr. Biol.* **164,** 103–114
44. Kuwabara, P. E., and Labouesse, M. (2002) *Trends Genet.* **18,** 193–201
45. Bretscher, M. S., and Munro, S. (1993) *Science* **261,** 1280–1281
46. Simons, K., and Toomre, D. (2000) *Nat. Rev. Mol. Cell. Biol.* **1,** 31–39
47. Castuma, C. E., Brenner, R. R., DeLucca-Gattas, E. A., Schreier, S., and Lamy-Freund, M. T. (1991) *Biochemistry* **30,** 9492–9497
48. Kimelberg, H. K. (1978) *Cryobiology* **15,** 222–226
49. Ge, M., Field, K. A., Aneja, R., Holowka, D., Baird, B., and Freed, J. H. (1999) *Biophys. J.* **77,** 925–933
50. Le Gall, S., Neuhof, A., and Rapoport, T. (2004) *Mol. Biol. Cell* **15,** 447–455
51. MacLennan, D. H., Rice, W. J., and Green, N. M. (1997) *J. Biol. Chem.* **272,** 28815–28818
52. Dhitavat, J., Dode, L., Leslie, N., Sakuntabhai, A., Lorette, G., and Hovnanian, A. (2003) *J. Investig. Dermatol.* **121,** 486–489
53. Hunter, G. W., Negash, S., and Squier, T. C. (1999) *Biochemistry* **38,** 1356–1364
54. Whiting, K. P., Restall, C. J., and Brain, P. F. (2000) *Life Sci.* **67,** 743–757
55. Squier, T. C., Bigelow, D. J., and Thomas, D. D. (1988) *J. Biol. Chem.* **263,** 9178–9186
56. Madden, T. D., Chapman, D., and Quinn, P. J. (1979) *Nature* **279,** 538–541
57. Johannsson, A., Keightley, C. A., Smith, G. A., and Metcalfe, J. C. (1981) *Biochem. J.* **196,** 505–511
58. Cheng, K. H., Lepock, J. R., Hui, S. W., and Yeagle, P. L. (1986) *J. Biol. Chem.* **261,** 5081–5087
59. Adams, C. M., Goldstein, J. L., and Brown, M. S. (2003) *Proc. Natl. Acad. Sci. U. S. A.* **100,** 10647–10652
60. Brown, A. J., Sun, L., Feramisco, J. D., Brown, M. S., and Goldstein, J. L. (2002) *Mol. Cell* **10,** 237–245
61. Zhang, Y., Yu, C., Liu, J., Spencer, T. A., Chang, C. C., and Chang, T. Y. (2003) *J. Biol. Chem.* **278,** 11642–11647
62. Chautan, M., Dell'Amico, M., Bourdeaux, M., Leonardi, J., Charbonnier, M., and Lafont, H. (1990) *Chem. Phys. Lipids* **54,** 25–32
63. Rodriguez, A., Bachorik, P. S., and Wee, S. B. (1999) *Arterioscler. Thromb. Vasc. Biol.* **19,** 2199–2206
64. Nilsson, I., Ohvo-Rekila, H., Slotte, J. P., Johnson, A. E., and von Heijne, G. (2001) *J. Biol. Chem.* **276,** 41748–41754